CRASHWORTHINESS ANALYSIS OF CIRCULAR AND SQUARE THIN-WALLED ALUMINUM AND HYBRID COMPOSITE TUBES

LÜTFIYE DAHIL * , KHALED NIMER MOHAMMED AL-NIMER

Department of Mechanical Engineering, Faculty of Engineering, Istanbul Aydin University, Küçükçekmece, 34295 Istanbul, Turkey

In the present study, crash simulations for thin-walled circular and square cross-section samples made of intra-layer glass-carbon/epoxy hybrid composite, and aluminum have been conducted; and energy absorption capacity and deformation modes are obtained. Results related to some post-collision parameters such as variation of displacement and force are presented for each combination of cross-sectional geometry and material, as well. Numerical method is validated by a previous experimental drop-weight study. Numerical calculations have shown that the hybrid composite sample of square cross-section exhibits the highest load resistance and maximum crash energy absorption, while aluminum samples have a low load resistance and energy absorption capacity the circular Al samples have smaller displacement than that of the square samples.

Keywords: *Intra-layer hybrid composites, numerical modeling, drop weight impact test, folding.*

1. Introduction

Composite materials are produced by addition of at least one type of reinforcement to the matrix phase and used in industrial applications widely owing to their relatively higher strength-to-weight ratio, modulus, and damping capability, as well as corrosive and electrical resistance. Hybrid composites use more than one type of reinforcement with different physical and chemical properties in the same matrix. With hybrid composites, it is possible to have greater control on properties, balancing the advantages and disadvantages of various reinforcement materials. In general, reinforcement of a high modulus, such as carbon and boron, and that of low modulus, such as E-glass and Kevlar, are combined in hybrid composites [1-3]. Four types of hybrid composites in the study as follow; “inter-ply hybrid composites” that consists of change fiber types in different distribution, “intra-ply hybrid composites” that consist two or more types of fibers used in the same layer, “inter-ply/intra-ply hybrid composites” that consists of inter-ply and intra-ply layers subjected in a exist distribution, and “resin hybrid composites” that can be built by using two or more resins rather than altering the fiber types [4]. It is important to analyze the crashworthiness of hollow structures of transportation vehicles before they are implemented in real life applications. Employing structural members made of hybrid composites reduce the total weight of the vehicle, keeping the crashworthiness at high levels [5]. Energy absorption capacity of glass epoxy resin and carbon epoxy resin composites are experimentally studied [6]. It is seen that the use of energy absorbing composite (EACS) structures in crash resistance application has been adopted by researchers. Energy-absorbing composite materials in aircraft, ships, wind turbines, automobiles and space applications are more advantageous than metallic materials due to their environmental friendliness and lightness [7, 8]. Since energy absorption depends on many parameters such as fiber type, matrix type, fiber orientation, sample geometry, processing conditions, fiber volume ratio and test speed, energy absorption in polymer composite materials had been investigated [9]. The front samples were designed to improve the performance of the collision and its structural mass was reduced, and then the crash test was conducted by FEA. Then the same test was conducted dynamically, and it was noted that the differences are small and changing the dimensions of the front samples greatly affects the crash performance [10]. Hybrid compounds consisting of several materials have become of great importance due to their mechanical properties such as light weight, the impact test was applied to the hybrid sample consisting of aluminum and steel and compared it with the same sample, but once for aluminum and again for steel, and it was noted that the hybrid sample is able to reduce Greater strength and enhanced energy absorption at the same time than a single substance [11]. Energy-absorption systems used in cars or whatever to vanish the impact energy along impact operation, that’s ensure

*Autor corespondent/*Corresponding author*,
E-mail: lutfiyedahil@aydin.edu.tr

the safety for the passengers, and one of the main energy absorption systems are the front rails [12.] Thin-walled structures are heavily used in automotive engineering as a frontal rail to vanish the impact against front impacts, and the capacity of materials are different while the requirements for energy absorption changes by the change of impact area rails [13]. Hybrid composite is presents that the crashworthiness and light weight of aluminum-steel material, and as a result for this test the hybrid composite materials increase the sum of absorbed forces by 117.83% and decrease the maximum force and mass by 16% and 7.73%, respectively [14]. While the simulation is heavily used for crashworthiness applications, it is usually noted that the accuracy of the simulations mainly depends on the number of elements [15]. Alternative models are used to make the performance of the impact process better on crashworthiness while reducing the total mass, in this study all scenarios of frontal rails like front crash on side crash have been analyzed [16]. The low velocity impact test represents that the impact force with respect to time for hybrid composites are oriented to different stacking ways. When the load starts, the velocity increases with displacement linearly, and makes the high velocity. After that, the unloading level starts, which present the nonlinear behavior [17]. Numerical and experimental results of the impact force with respect to time and absorbed energy with respect to time relationships for impact energy were compared. These results when composed are very close to each other [18]. Carbon epoxy resin and glass epoxy resin laminates were subjected to low velocity impact loading for comparison to hybrid samples. In the event of impact, energy is absorbed from new surfaces formed through elastic deformation, plastic deformation, and fracture. [19]. It is important to analyze the crashworthiness of hollow structures of transportation vehicles before they are implemented in real life applications. Employing structural members made of hybrid composites reduce the total weight of the vehicle, keeping the crashworthiness at high levels [20]. Researchers' attention has turned to improving the durability of FRF composites as structural members are capable of absorbing large amounts of impact energy while gradually collapsing in a controlled manner. FRP composite structures do not deform plastically when subjected to compressive loads, but collapse in various modes, with developing extensive micro-cracking as the predominant damage mechanism [21-27].

Main purpose of the present study is to compare energy absorption capacity and deformation modes of circular and square cross-section samples made of intra-layer hybrid composites and aluminum, numerically. For validation purpose, results of the numerical drop weight test, which is conducted for unidirectional hybrid carbon-glass/epoxy composite in the present study, are compared with those of a previous experimental study [28]. Then, finite element models of samples of square and circular cross-section made of intra-layer hybrid composite and aluminum are created, and several crashworthiness tests are conducted. Results of the numerical calculations are presented in terms of variation of force and displacement with time; as well as that of with displacement, for the first six folds.

2. The numerical method

2.1 Materials

In the numerical crash simulations, samples of circular and square cross-sections made of A2014-T6 aluminum alloy and intra-layer hybrid carbon-glass/epoxy composite are used. Some mechanical properties of aluminum alloy and the components that make up the hybrid composite are given in Table 1.

Numerical model of the intra-layer hybrid composite material is created using ANSYS Material Designer, where unidirectional carbon and glass fibers are dispersed in an epoxy resin matrix. To create the intra-layer hybrid composite model,

Table 1

Some mechanical properties of the materials used in the numerical calculations

Material	Tensile Strength (MPa)	Elasticity Modulus (GPa)	Strain (%)	Density (g/cm^3)
A2014-T6 aluminum alloy	450-485	73	13	2.8
Carbon (TORAY) T620SC-24K-50C	4400	235.0	1.7	1.77
E-cam (CPIC) ECT469L-2400	1838	73.1	4.51	2.54
Epoxy Resin	75	3.10	5.26	1.13

Table 2

CG intra material properties (Moduli of elasticity E, Poisson Ratio V́, Shear Stress Ꞇ)

Density (ρ) (kg/m^3)	Moduli of elasticity [MPa]			Poisson ratio			Shear moduli [MPa]		
	E_1	E_2	E_3	ν_1	ν_2	ν_3	τ_1	τ_2	τ_3
1697.7	71340.1	7155.4	7155.4	0.3	0.5	0.3	2620.3	2443.1	2620.3

first, carbon and glass fibers are combined with a volume fraction of 50% and a fiber diameter of 0.5 µm. Afterwards, the fiber mixture is combined with epoxy resin and the final composite material model shown in Fig. 1 is obtained. Then, mechanical properties of the hybrid composite material are calculated by the software, which are presented in Table 2. These values are further used as input parameters in the ABAQUS, for impact and crash tests.

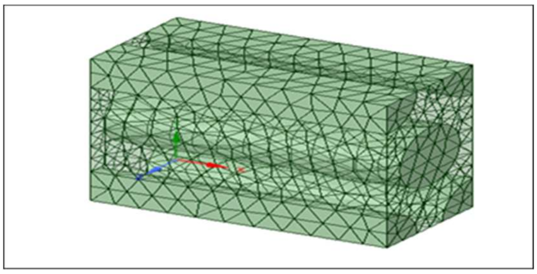

Fig. 1 - The numerical model of intra-layer hybrid composite material

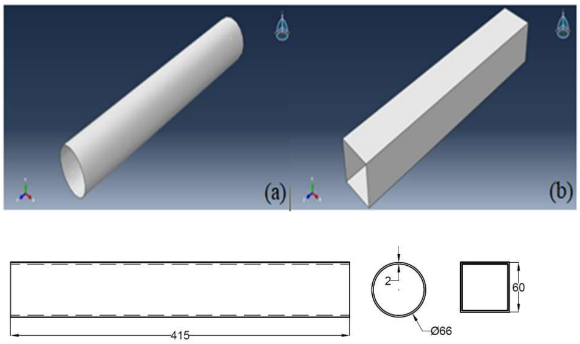

c.

Fig. 2 - Illustration of model geometries for samples of **a)** circular cross-section, **b)** square cross-section; as well as **c)** relevant dimensional parameters (in mm)

2.2 Geometry, Mesh and Boundary Conditions

Geometrical models of the samples are created using ABAQUS which are shown in Fig. 2. Length and thickness of the samples are L = 415 mm, and t = 2 mm, respectively; while diameter of the circular sample is D = 66 mm and edge length of the square is a = 60 mm (Fig. 2c).

Figure 3 illustrates the numerical grid used in the calculations, which have approximately 1800 elements. The boundary conditions employed in the crash simulations are shown in Fig. 4 schematically. Accordingly, the front end of the sample is fixed, which is taken as the reference plane. The impactor used in the crash simulations is a rigid wall with a mass of 500 kg, moving in the axial direction of the samples with a velocity of 36 km/h. Time period of the crash tests is 0.05 s.

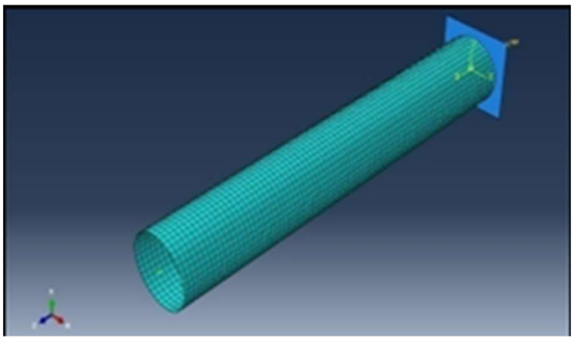

Fig. 3 - Numerical grid (mesh)

2.3 Validation

To validate the numerical method used in the present study, results of the drop weight impact test are used in the previous experimental study by Pashmforoush [28], where the Hashin' s criteria is employed to study the damage resistance behavior of unidirectional carbon fibers in epoxy under impact. Crash simulations are conducted using the ABAQUS solver which employs the finite element method (FEM). A semi-spherical rigid ball is used as impactor, in compliance with the ASTM D7136 standard, while the initial velocity and mass of the ball is 4 m/s and 2 kg, respectively [28]. The

Table 3

Impact force and displacement values of numerical and experimental impact tests

Solution	Force [MPa]	Numerical Displacement [mm]	Experimental Displacement [mm] [28]	[%]
S1	200	3.6	3.58	0.5
S2	300	4.51	4.26	5.9
S3	400	4.88	4.87	0.2

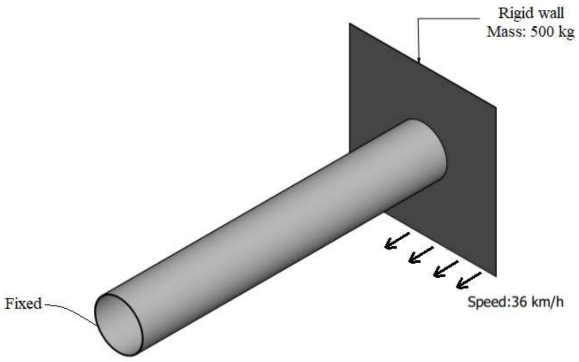

Fig. 4 - Illustration of the boundary conditions

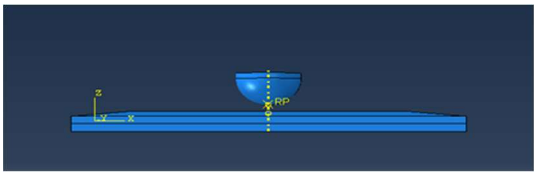

a.

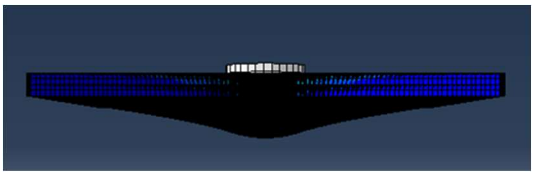

b.

Fig. 5 - Illustration of **a)** the numerical model of the impact test specimen, and **b)** displacement after impact

numerical model of the impact test setup, and displacement after impact is shown in Figs. 5a and 5b, respectively. As seen in Table 3, results of the numerical drop weight test are found to agree well with those of the experimental study with a maximum deviation of less than 6 %.

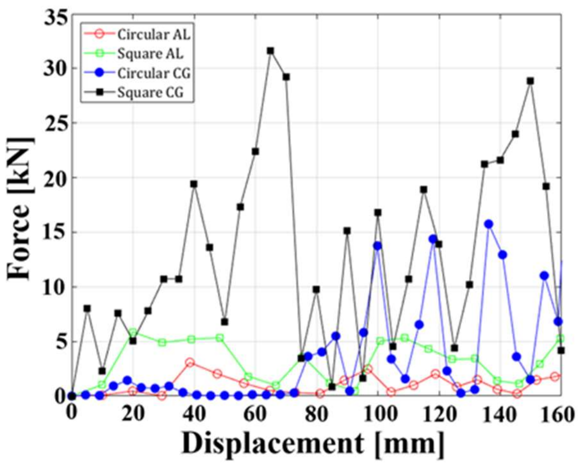

Fig. 6 - Force - displacement curves for all types of materials

3. Results and discussion

In the numerical crash simulations effect of material properties and cross-sectional geometry on the energy absorbed, and deformation modes exhibited by aluminum and hybrid composite samples are investigated. Results related to some post-collision parameters such as displacement, force, and amount of dissipated energy are presented for each combination of cross-sectional geometry and material.

Figure 6 presents a comparison of force-displacement curves for each type of materials for at least the first four folding modes, which can generally be identified by some decrease in modulus of elasticity followed by an increase. It can readily be observed that the hybrid composite sample of square cross-section exhibits the highest load resistance. On the contrary, hybrid composite sample of circular cross-section deforms under much smaller load at the initial stages of loading, whereas its load resistance increases beyond some value of displacement and approaches to that of square cross-section. Aluminum samples have a low load resistance for overall process and show a relatively more stable load response, regardless of their cross-sectional profile. Characteristic point data for the first six folding are presented in Fig. 7. Accordingly, value of force corresponding the first folding is the highest for the hybrid composite sample of square cross-section, followed by that of Al sample of square cross-section, while there is a negligible difference between the first-folding force values of the samples of circular cross-section (Fig. 7a). Also, the first folding is delayed for the hybrid composite sample of square cross-section as the first folding occurs approximately at the same instant for the rest of the materials (Fig. 7b-c). The total absorbed energy can be obtained by the area under the force-displacement curves, which is presented in Fig. 8. Thus, it is seen that the hybrid composite of square cross-section absorbs maximum energy, whereas the samples made of aluminum absorb collision energy the least. Also, it is seen that samples of square cross-section absorbs more energy than those of circular one, which is reported to be due to an increase of the number of folds and plastic hinges for square cross-section [29].

Time variation of displacement is shown in Fig. 9. It is seen that displacement curves of the hybrid composite samples are close to each other and linear, whereas aluminum samples have a non-linear displacement-time curve. The hybrid composite sample of circular cross-section shows minimum deformation per unit time, followed by that of square cross-section, while aluminum samples exhibit relatively larger displacement in time. Therefore, it can be said that hybrid composite samples are safer than aluminum samples.

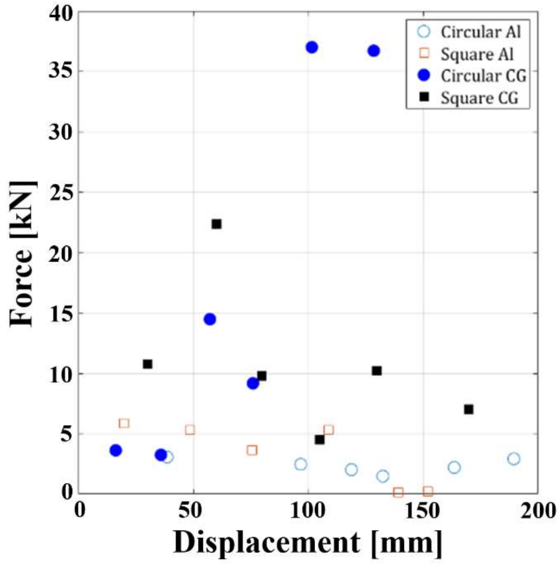

a

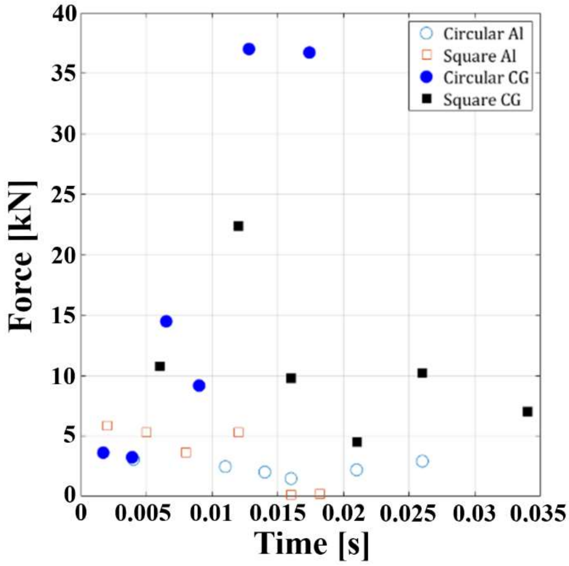

b

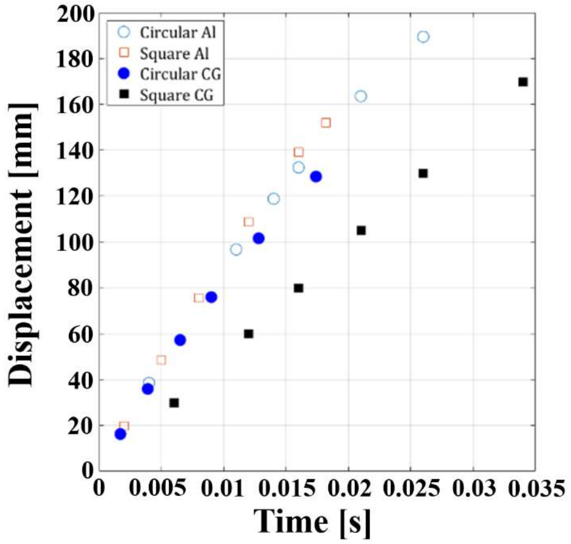

c

Fig. 7 - Characteristic point values of **a)** force-displacement, **b)** force-time, and **c)** displacement-time; related to the first six modes of folding

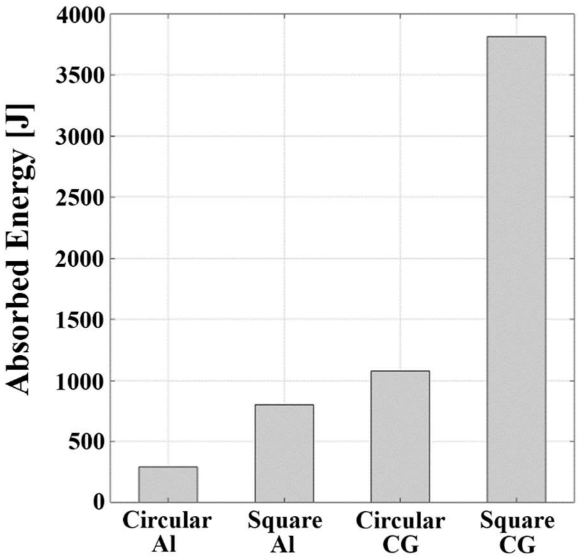

Fig. 8 **-** Total absorbed energy for all types of materials

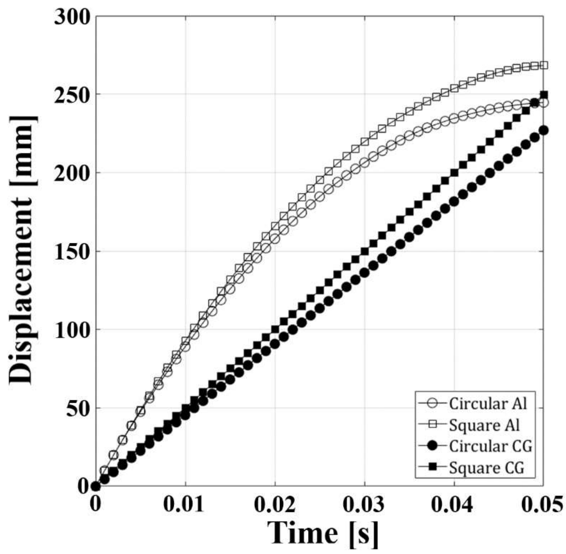

Fig. 9 **-** Variation of displacement with time

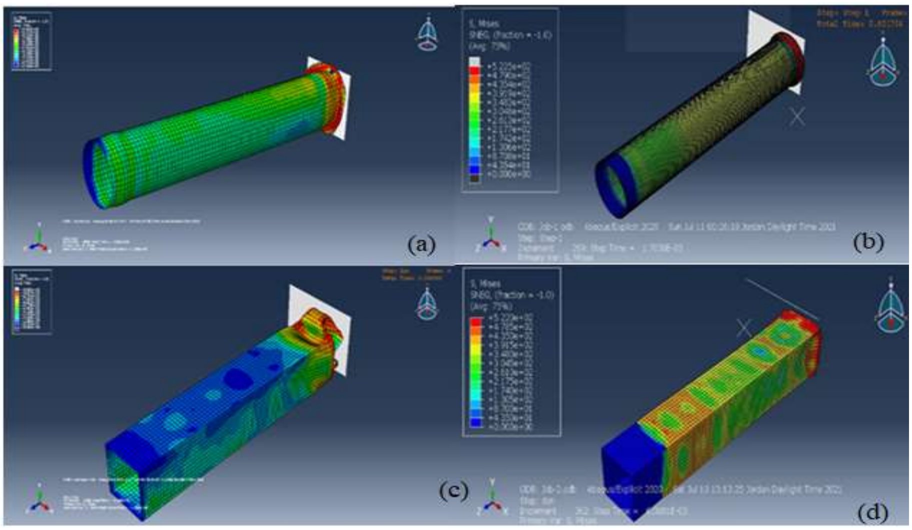

Fig. 10 **-** Deformation after folding Mode I superimposed with contour plots of von Mises stress: **a)** circular Al, **b)** circular CG, **c)** square Al, **d)** square CG

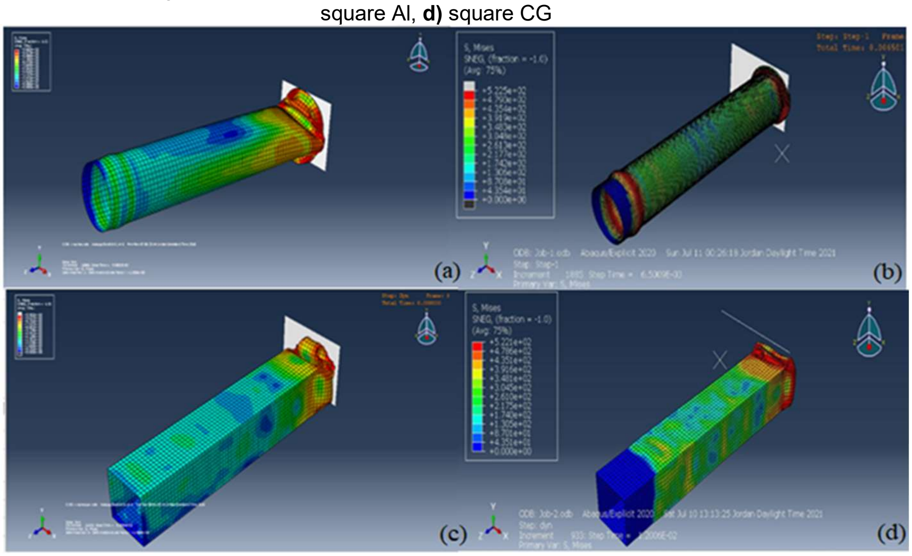

Fig. 11 **-** Deformation after folding Mode II superimposed with contour plots of von Mises stress: **a)** circular Al, **b)** circular CG, **c)** square Al, **d)** square CG

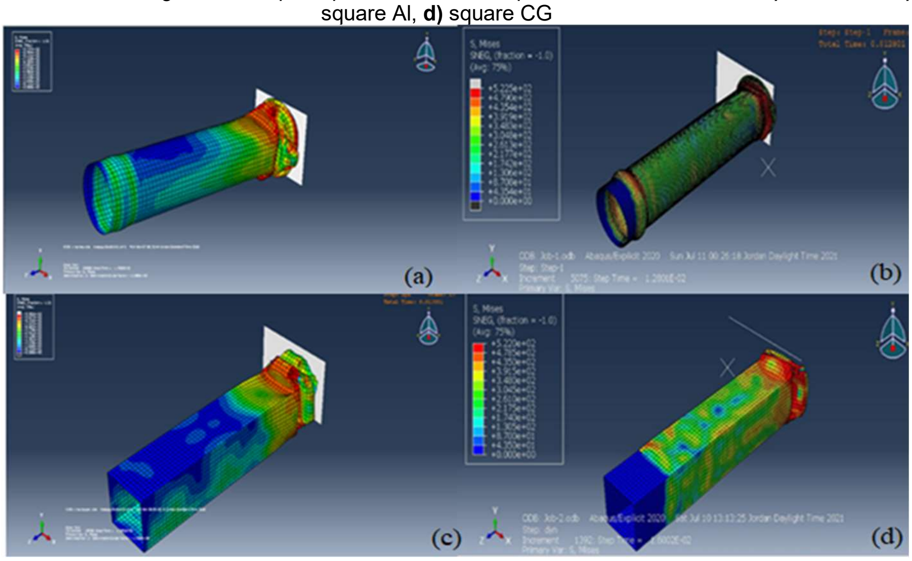

Fig. 12 **-** Deformation after folding Mode III superimposed with contour plots of von Mises stress: **a)** circular Al, **b)** circular CG, **c)** square Al, **d)** square CG

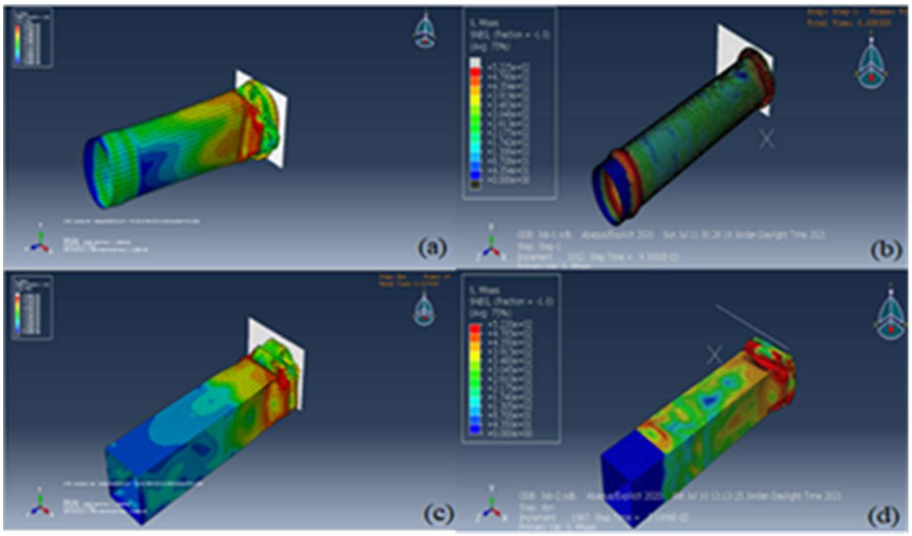

Fig. 13 - Deformation after folding Mode IV superimposed with contour plots of von Mises stress: **a)** circular Al, **b)** circular CG, **c)** square Al, **d)** square CG

Deformation and contour plots of von Mises stress are illustrated in Figs. 10-13 for the first four folding modes. It is reported that for circular tubes of diameter-to-thickness ratio $D/t < 50$, and length-to-thickness ratio $L/t > 2$, as well as for square tubes of edge-to-thickness ratio within the range $7.5 \leq a/t \leq 40.8$; mixed mode folding, i.e., both diamond mode and ring mode, is expected [30]; which is already observed in Figs. 10-13. An axisymmetric folding is apparent near the front end of the circular samples (Figs. 10a-b, 11a-b, 12a-b, and 13a-b). It is remarkable that square Al sample folds both inward and outward at the first folding, whereas the others exhibit a folding outward.

4. Conclusion

In the present study, crash simulations for thin-walled circular and square cross-section samples made of intra-layer glass-carbon/epoxy hybrid composite, and aluminum have been conducted; and energy absorption capacity and deformation modes are obtained. Results related to some post-collision parameters such as variation of displacement and force are presented for each combination of cross-sectional geometry and material, as well. Numerical method is validated by a previous experimental drop-weight study.

Significant outcomes of the numerical calculations are as follows:

- The hybrid composite sample of square cross-section exhibits the highest load resistance, while aluminum samples have a low load resistance for overall process and show a relatively more stable load response, regardless of their cross-sectional profile.

- The hybrid composite of square cross-section absorbs maximum energy, whereas the samples made of aluminum absorb collision energy the least.

- Samples of square cross-section absorbs more energy than those of circular one, which is expected.

- Mixed mode folding is observed for all samples, which is expected due to the diameter-to-thickness and edge length-to-thickness ratios of the circular and square cross-sectional samples.

REFERENCES

[1] J. O'Donnell and V. Chalivendra, Multi-functional glass/carbon fibers hybrid inter/intra laminated composites, Composites Part C: Open Access, 2021; **4**; 100121.

[2] R.D. Cunha, R.A.D. da Cunha, W.F. de Amorim Junior, R. C. S. Freire Júnior, Study of the Resistance Variation in Intraply/Yarn Kevlar/Glass Composite after Low-Velocity Impact, Journal of Materials Engineering and Performance, 2020; **29**(8); 5001-5007.

[3] N. Hashim, D. L. A. Majid, E. S. Mahdi, R. Zahari and N. Yidris, Effect of fiber loading directions on the low cycle fatigue of intraply carbon-Kevlar reinforced epoxy hybrid composites, Composite Structures, 2019; **212**; 476-483.

[4] Ç. Uzay, D. C. Acer and N. Geren, Impact strength of interply and intraply hybrid laminates based on carbon-aramid/epoxy composites, European Mechanical Science, 2019, **3**(1),1-5.

[5] M. Kathiresan, K. Manisekar and V. Manikandan, Crashworthiness analysis of glass fibre/epoxy laminated thin-walled composite conical frusta under axial compression, Composite Structures, 2014; **108**, 584-599.

[6] S. Ochelski and P. Gotowicki, Experimental assessment of energy absorption capability of carbon-epoxy and glass-epoxy composites, Composite Structures, 2009; **87**(3), 215-224.

[7] C. W. Isaac, M. Pawelczyk and S. Wrona, Comparative study of sound transmission losses of sandwich composite double panel walls, Applied Sciences, 2020; **10**(4), 1543.

[8] C. W. Isaac and C. Ezekwem, A review of the crashworthiness performance of energy absorbing composite structure within the context of materials, manufacturing and maintenance for sustainability, Composite Structures, 2021; **257**: 113081.

[9] G. C. Jacob, J. F. Fellers, S. Simunovic and J. M. Starbuck, Energy absorption in polymer composites for automotive crashworthiness, Journal of composite materials, 2002; **36**(7), 813-850.

[10] Q. Q. Li, E. Li, T. Chen, L. Wu, G. Q. Wang and Z. C. He, Improve the frontal crashworthiness of vehicle through the design of front rail, Thin-Walled Structures, 2021; **162**: 107588.

[11] J. Fang, N. Qiu, X. An, F. Xiong, G. Sun and Q. Li, Crashworthiness design of a steel–aluminum hybrid rail using multi-response objective-oriented sequential optimization, Advances in Engineering Software, 2017; **112**
, 192-199.

[12] Y. Wu, J. Fang, Z. Cheng, Y. He and W. Li, Crashworthiness of tailored-property multi-cell tubular structures under axial crushing and lateral bending, Thin-Walled Structures, 2020; **149**: 106640.

[13] Y. Shi, P. Zhu, L. Shen and Z. Lin, Lightweight design of automotive front side rails with TWB concept, Thin-walled structures, 2007; **45**(1), 8-14.

[14] Y. Zhou, F. Lan and J. Chen, Crashworthiness research on S-shaped front rails made of steel–aluminum hybrid materials, Thin-Walled Structures, 2011; **49**(2), 291-297.

[15] J. Fang, Y. Gao, G. Sun, Y. Zhang and Q. Li, Crashworthiness design of foam-filled bitubal structures with uncertainty, International Journal of Non-Linear Mechanics, 2014; **67**, 120-132.

[16] M. Kiani and A. R. Yildiz, A comparative study of non-traditional methods for vehicle crashworthiness and NVH optimization, Archives of Computational Methods in Engineering, 2016; **23**(4), 723-734.

[17] A. Güneş and Ö. S. Şahin, Effect of surface crack depth on hybrid laminated composites, Arch Mater Sci Eng, 2016; **82**(1), 38-41.

[18] W. He, J. Liu, B. Tao, D. Xie, J. Liu and M. Zhang, Experimental and numerical research on the low velocity impact behavior of hybrid corrugated core sandwich structures, Composite Structures, 2016; **158**, 30-43.

[19] M. V. Hosur, M. Adbullah and S. Jeelani, Studies on the low-velocity impact response of woven hybrid composites, Composite Structures, 2005; **67**(3), 253-262.

[20] M. Kathiresan, K. Manisekar and V. Manikandan, Crashworthiness analysis of glass fibre/epoxy laminated thin-walled composite conical frusta under axial compression, Composite Structures, 2014; **108**, 584-599.

[21] A. G. Mamalis, D. E. Manolakos, M. B. Ioannidis and D. P. Papapostolou, Crashworthy characteristics of axially statically compressed thin-walled square CFRP composite tubes: experimental, Composite Structures, 2004; **63**(3-4), 347-360.

[22] D. Hull, A unified approach to progressive crushing of fibre-reinforced composite tubes, Composites science and technology, 1991; **40**(4), 377-421.

[23] G. L. Farley and R. M. Jones, Crushing characteristics of continuous fiber-reinforced composite tubes, Journal of composite Materials, 1992; **26**(1), 37-50.

[24] A. H. Fairfull, Energy absorption of polymer matrix composite structures: frictional effects, In: Wierzbicki T, Jones N. (eds.) Structural failure, Wiley-Interscience, 1989.

[25] A. G. Mamalis, D. E. Manolakos and G. L. Viegelahn, Crashworthy behaviour of thin-walled tubes of fibreglass composite materials subjected to axial loading, Journal of Composite Materials, 1990; **24**(1), 72-91.

[26] A. G. Mamalis, Y. B. Yuan and G. L. Viegelahn, Collapse of thin–wall composite sections subjected to high speed axial loading, International journal of vehicle design, 1992; **13**(5-6), 564-579.

[27] A. G. Mamalis, D. E. Manolakos, G. A. Demosthenous and M. B. Ioannidis, Analysis of failure mechanisms observed in axial collapse of thin-walled circular fibreglass composite tubes, Thin-Walled Structures, 1996; **24**(4), 335-352.

[28] F. Pashmforoush, Finite element analysis of low velocity impact on carbon fibers/carbon nanotubes reinforced polymer composites, Journal of Applied and Computational Mechanics, 2020; **6**(3), 383-393.

[29] A. A. Nia and J. H. Hamedani, Comparative analysis of energy absorption and deformations of thin walled tubes with various section geometries, Thin-Walled Structures, 2010; **48**(12), 946-954.

[30] A. Baroutaji, M. Sajjia and A. G. Olabi, On the crashworthiness performance of thin-walled energy absorbers: recent advances and future developments, Thin-Walled Structures, 2017; **118**, 137-163.

****